Magnetic Form Factor of Co^{++} Ion in Cobaltous Oxide

D. C. KHAN
Department of Physics, Indian Institute of Technology, Kanpur, India

AND

R. A. ERICKSON
Department of Physics, Ohio State University, Columbus, Ohio

(Received 25 August 1969)

The van Laar model of the spin structure of CoO in the antiferromagnetic state is supported on the basis of neutron-diffraction data from a single crystal. Then, the magnetic form factor of the Co^{++} ion in CoO is calculated. The anisotropic part of the form factor is studied in detail to arrive at the ground-state electron configuration of the Co^{++} ion. The spherical form factor is determined and plotted as a function of $(\sin\theta)/\lambda$ and compared with the theoretical form-factor curve. Attempts have been made to give some qualitative explanation of the deviation from the theoretical curve. Finally, conclusive evidence is put forward for discarding Roth's collinear model and Li's model from an analysis of the form-factor curves based on them.

INTRODUCTION

UNPAIRED electrons of the unfilled $3d$ shell of the iron-transition-series elements account for many of their important physical properties. So the determination of the charge distribution of these $3d$ electrons has been the concern of many theoretical and experimental investigations. Since the magnetic form factor is a direct measure of the charge density distribution of these unpaired electrons, accurately determined form factors are of great importance. In the last decade the study has been extended to the case of transition-series ions in crystalline environments. Weiss and Freeman[1] have calculated the effect of the nonspherical charge distributions of d and f electrons in cubic, tetragonal, and hexagonal crystalline fields on form factors. Their theory indicates that large deviations from the usual spherically symmetric approximations are to be expected and that these deviations lead to a new method for determining the spatial symmetry of the outer electrons in crystalline fields. Watson and Freeman's[2] calculations of the individual $3d$ transforms using accurate Hartree-Fock self-consistent field wave functions in conjunction with Weiss and Freeman's theory provide a very suitable background for the experimental study of the form factors.

In the present work, the properties of cobaltous oxide in its antiferromagnetic state have been studied by neutron diffraction, leading to an experimental determination of the magnetic form factor of the Co^{++} ion therein.

MODELS FOR SPIN STRUCTURE

Calculation of the form factor from the diffracted neutron intensity requires a knowledge of the spin structure in the crystal. The spin assignment in CoO in the antiferromagnetic state, i.e., below the Néel temperature of 293°K, has, however, recently reached a controversial stage.[3–8] Li[9] proposed two models, model A and model B, based on the assumption of a single magnetic axis (Fig. 1). Model A is characterized by the fact that the crystallographically unique (111) planes are ferromagnetic sheets and the alternate (111) planes have parallel and antiparallel arrangements of their spin. From powder-diffraction data, Shull *et al.*[10] as well as Roth[11] accepted model A. Roth assigned the spin direction parallel to $[\bar{1}\bar{1}7]$, which makes an angle 11°30′ with respect to [001]. Nagamiya and Motizuki[12] theoretically arrived at a similar result (angle of deviation 10°). Roth[13] later introduced a number of multispin axis structures (I,K,R,T,U) with tetragonal symmetry in

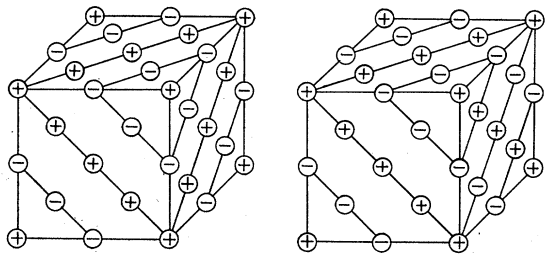

FIG. 1. Li's models A and B. Circles with + sign represent Co^{++} ion with spin-up. Circles with − sign represent that with spin-down.

[1] R. J. Weiss and A. J. Freeman, J. Chem. Phys. Solids **10**, 147 (1959).
[2] R. E. Watson and A. J. Freeman, Acta Cryst. **14**, 27 (1961).
[3] E. Uchida, N. Fukuoka, H. Kondoh, T. Takeda, Y. Nakazumi, and T. Nagamija, J. Phys. Soc. Japan **19**, 2088 (1964).
[4] B. van Laar, J. Phys. Soc. Japan **20**, 1282 (1965).
[5] T. Nagamija, S. Saito, Y. Shimomura, and E. Uchida, J. Phys. Soc. Japan **20**, 1285 (1965).
[6] J. H. Greiner, A. E. Berkowitz, and J. E. Weidenborner, J. Appl. Phys. **37**, 2149 (1966).
[7] S. Saito, K. Nakahigashi, and Y. Shimomura. J. Phys. Soc. Japan **21**, 850 (1966).
[8] H. N. Ok and J. G. Mullen, Phys. Rev. **168**, 563 (1968).
[9] Y. Y. Li, Phys. Rev. **100**, 627 (1955).
[10] C. G. Shull, W. A. Strausar, and E. O. Wollan, Phys. Rev. **81**, 333 (1951).
[11] W. L. Roth, Phys. Rev. **110**, 1333 (1958).
[12] T. Nagamiya and K. Motizuki, Rev. Mod. Phys. **30**, 89 (1958).
[13] W. L. Roth, Phys. Rev. **111**, 772 (1958).

keeping with the tetragonal distortion[14] of CoO in the antiferromagnetic state, which were in concordance with his powder-diffraction data. Recently, van Laar[15] repeated Roth's experiment with a high-resolution diffractometer and rejected Roth's multispin models *I*, *K*, *R*, *U*, *T* as well as his uniaxial spin assignment [$\bar{1}\bar{1}7$]. He could explain these data as well as his single-crystal diffraction data[16] with a collinear model *A* with an angle of deviation of 27.4° ($\alpha=-0.325$, $\beta=-0.325$, $\gamma=+0.888$) or equally well with a multispin axis structure described in Table I. He preferred the multispin model because of its strict tetragonality.

On the other hand, Uchida *et al.*[3] interpreted their recent magnetic anisotropy measurements in terms of Roth's single-axis model *A* with spin along [$\bar{1}\bar{1}7$]. Greiner, Berkowitz, and Weidenborner[6] studied the torque curves of single-crystal CoO films after cooling them down in a magnetic field of 20 kOe. They rule out the multispin-axis van Laar model and decide in favor of the collinear model with the spin axis making an angle of 27.4° with the *c* axis as the only possible arrangement of spins in CoO. Again, Saito *et al.*[7] found that their low-temperature x-ray diffraction data could best be explained by Roth's collinear model with the spin axis making an angle of 10° with the *c* axis. Recently, Ok and Mullen[8] concluded from the analysis of Mössbauer hyperfine spectra that in the case of vacancy-free CoO, called CoO(I) by them, the spin arrangement agrees with the van Laar model. This situation makes it imperative to come to a conclusion about the spin structure from the present experimental data before the final assignment of the form-factor values.

EXPERIMENTAL

The CoO crystal used for the present study was kindly supplied by Dr. Y. Nakazumi of Tochigi Chemical Industrial Co., Osaka, Japan, who grew the crystal by the flame-fusion method. The crystal was first cut and polished to an approximate cube 6.01×6.03×6.06 mm in size with faces perpendicular to [001], [110], and [1$\bar{1}$0] directions. Then we attempted to make the crystal spherical. This was necessitated by the boundary conditions of the numerical integration method used for absorption-extinction corrections. Following a technique due to Bond,[17,18] corners were rounded off, but the process was not continued to completion, as parallel dummy experiments suggested that there was a possibility of the crystal breaking up along a cleavage plane.

The crystal was mounted on a commercial two-stage thermoelectric cooler. The cooler itself was mounted on a GE orienter fixed to a cast-aluminum holder so that the orienter could have an oscillatory motion about a horizontal axis by means of a cam arrangement.

A practical technique[19] was developed for the coincident reflection correction. The crystal was continually oscillated about the scattering vector by the above-mentioned arrangement during an intensity measurement, thus, averaging over the *umweganregung* and *aufhellung* peaks, if present, and bringing the average intensity close to the true intensity.

The temperature of the cooler is a continuous function of the current sent through it. The minimum temperature attainable was −45°C.

TABLE I. van Laar's multispin model of CoO.

Origin of sublattice	Direction cosines of spins		
	α	β	γ
1. 0 0 0	−0.325	−0.325	+0.888
2. $\frac{1}{4}$ 0 $\frac{1}{4}$	+0.325	−0.325	−0.888
3. $\frac{1}{4}$ $\frac{3}{4}$ $\frac{1}{4}$	+0.325	+0.325	+0.888
4. 0 $\frac{3}{4}$ $\frac{3}{4}$	−0.325	+0.325	−0.888

CORRECTION FACTORS AND EXPERIMENTAL PARAMETERS

The (111) peak was studied as a function of temperature through the cooler range as well as at 77°K by mounting the crystal in a liquid-nitrogen vacuum cryostat. The intensity-versus-temperature curve was extrapolated to 0°K. Most of the peaks were studied around −40°C, and the intensities corrected with the help of this curve to get the diffracted intensity at saturation magnetization.

Zachariasen's extinction correction formula[20,21] could not be used because the present experimental set up did not allow measurements at two different wavelengths. An IBM 709/7090 SCATRAN program was developed for the calculation of the absorption-extinction correction by adopting Hamilton's method[22] to the case of a spherical surface. The value of η, the mosaic spread parameter, found by utilizing the intensity ratios of the nuclear peaks (222), (044), and (444), was five minutes of arc. The extinction correction was neglected for peaks with extremely low intensities [peaks with integrated intensities less than 1% of the integrated intensity of the (111) peak]. However, since the experimental crystal was not a perfect sphere, correction factors could not be exact and this introduced a minor uncertainty in the analysis as revealed in the somewhat broad erorr limits. The value of the $2B$ term of the Debye-Waller factor at 233°K was determined to be 1.00×10^{-16} cm^2 from a study of the integrated intensities of the nuclear peaks (222), (004), (044), (444), and (666). The value of $2B$ at 77°K was found by comparison of the inte-

[14] N. C. Tombs and H. P. Rooksby, Nature **165**, 442 (1950).
[15] B. van Laar, Phys. Rev. **138**, A584 (1965).
[16] B. van Laar, J. Schweizer, and R. Lemaire, Phys. Rev. **141**, 538 (1966).
[17] W. L. Bond, Rev. Sci. Instr. **22**, 344 (1951).
[18] W. L. Bond, Rev. Sci. Instr. **25**, 401 (1954).
[19] D. C. Khan and R. A. Erickson, Rev. Sci. Instr. **41**, 107 (1970).
[20] W. H. Zachariasen, Phys. Rev. Letters **18**, 193 (1967).
[21] W. H. Zachariasen, Acta Cryst. **23**, 558 (1967).
[22] W. C. Hamilton, Acta Cryst. **16**, 609 (1963).

grated intensities of the (222) and (444) peaks at 233 and 77°K to be 0.46×10^{-16} cm². The values are low compared to the thermal vibration factors due to Roth[11] and van Laar[15] ($2B=1.00\times10^{-6}$ cm² at 4°K and $2B=0.74\times10^{-16}$ cm² at 77°K, respectively). However, the range of $(\sin\theta)/\lambda$ covered by their data was only about half of that covered in the present experiment.

The wavelength of the incident beam was determined from a preliminary experiment to be $\lambda=0.9587\pm0.0084$ Å with 0.3% $\frac{1}{2}\lambda$ component. Each (h,k,l) peak power was corrected by this factor of the power of the $(2h,2k,2l)$ peak.

The validity of these values of different experimentally determined parameters can be demonstrated by calculating the crystal structure factors for the various nuclear peaks from the experimental integrated intensities and comparing them with the theoretically calculated structure factors (Table II).

DOMAIN STRUCTURE AND SPIN STRUCTURE

In model B or in the van Laar model antiferromagnetic domains result if there is a rotation of the direction of the moments or moment sets, respectively, with respect to each other (referred to as S domains in the following). In model A antiferromagnetic domains result if there is a rotation of the direction of moments between the ions in the ferromagnetic sheet (S domains) or if there is a change in the crystallographic orientation of the ferromagnetic sheets (referred to as T domains). There are three types of S domains corresponding to the three tetragonal contraction axes, and four T domains corresponding to four rhombohedral contraction axes. In general, there will be twelve fractional-domain volume coefficients $C_s{}^t$ ($t=1$ to 4, $S=1$ to 3) in generalized q^2 term[23] in the diffracted intensity expression. The value of the generalized q^2 term will depend on the spin structure and the value of the coefficients $C_s{}^t$, usually affecting differently even the individual peaks (hkl) of a set $\{hkl\}$.

Table III gives the experimental results for the {111} set. Model A will explain this equality of the {111} peaks with the assumption that each of the T domains is of exactly equal volume. Any distribution of S domains in model A, B, or van Laar model will be consistent with these data.

TABLE II. Comparison of experimental and theoretical structure factors: $|F_{\text{nucl}}|$.

Peak	$\lvert F_{\text{nucl}}\rvert$ (10^{-12} cm) Calculated	Observed
222	10.46	10.39
004	26.46	26.08
044	26.46	27.19
444	26.46	26.85
666	10.46	10.29

[23] G. E. Bacon, *Neutron Diffraction* (Oxford University Press, London, 1962), 2nd ed., p. 163.

TABLE III. Integrated intensities of {111} peaks.

Peak	Temperature	Integrated intensity (arbitrary units)
111	−40.5	123 792
$\bar{1}11$	−40.5	120 859
$1\bar{1}1$	−40.5	120 462
$11\bar{1}$	−40.5	120 694

Table IV gives the integrated intensities of the peaks in the {311} set. Model B and the van Laar model with three simple S-type domains explain the data excellently with $C_1=0.4$ and $C_2=C_3=0.3$. Model A will again explain the data with four equal T domains, each of them having two equal S domains and a third S domain of somewhat greater volume.

The observed intensity patterns of both {111} and {311} sets remained unchanged by thermal cycling through the Néel point in a condition free of external field effects. The repeated equality of the T domains, in spite of the thermal inhomogeneity of each cooling process, would be highly improbable. This strongly suggests that we should neglect model A. With regard to Model B, van Laar's powder data[24] for the intensity ratio of the resolved $\{311\}_t$ and $\{311\}_t$ peaks ruled it out as a possible model for the spin arrangement. Here $\{311\}_t$ represents the subset of the set of peaks {311}, each element of which has the same tetragonal form as the peak (311), whereas $\{113\}_t$ represents the subset, each element of which has the same tetragonal form as the peak (113). Hence, calculations for the magnetic form factor were carried out with the van Laar multiaxis model (Table I). However, in view of the present controversial stage of the problem, parallel calculations were made with Roth's model A with deviation angle of 10° supported by Saito *et al.*[7] and also with Li's model B. The enormous discrepancy of the results from the theoretical form factor was used as a decisive factor in favor of van Laar's model. Roth's model A with deviation angle of 27° supported by Greiner *et al.*[6] would formally yield the same results as van Laar's model. But, this could be discarded, because, apart from the general objection to model A discussed above, an angle of devia-

TABLE IV. Integrated intensities of {311} peaks.

Peak	Temperature (°C)	Integrated intensity (arbitrary units)	Peak	Temperature	Integrated intensity (arbitrary units)
311	−39.2	28 303	$1\bar{3}1$	−39.4	27 502
$\bar{3}11$	−39.3	27 138	$13\bar{1}$	−39.2	27 422
$3\bar{1}1$	−39.3	27 682	113	−39.2	23 666
$31\bar{1}$	−39.3	27 027	$\bar{1}13$	−39.4	23 166
131	−39.3	28 186	$11\bar{3}$	−39.4	23 382
$\bar{1}31$	−39.2	27 370	113	−39.0	23 486

[24] B. van Laar, Ph.D. thesis, University of Leiden, 1968 (unpublished).

tion as large as 27° would contradict the basic assumptions of the Nagamiya-Motizuki theory.[12]

ANISOTROPY IN THE FORM FACTOR

Figure 2 shows a typical diffraction pattern of CoO. The peaks are either purely nuclear or purely magnetic. The quantity $f\mu$ of the Co^{++} ion, where f is the relative magnetic form factor and μ is the magnetic moment in Bohr magnetons, was calculated for each magnetic peak and plotted against $(\sin\theta)/\lambda$, where λ is the neutron wavelength and θ is the Bragg angle. The intercept of a smooth curve, which fits the data for peaks at low $(\sin\theta)/\lambda$, at $(\sin\theta)/\lambda=0$ is 3.35 ± 0.04. This, by definition, is the value of μ. This is about 4% less than the value reported by van Laar.[15]

A plot of f as a function of $(\sin\theta)/\lambda$ showed that the experimental points at the same abscissa are split apart for large values of $(\sin\theta)/\lambda$. Hence, a monotonic isotropic form-factor function cannot fit the experimental data. This suggests the existence of a nonspherical charge distribution in the Co^{++} ion.

The electronic structure of the free Co^{++} ion in its ground state consists of an argon core plus seven $3d$ electrons and the structure can be described as a $^4F_{9/2}$ state. In the CoO crystal, the Co^{++} ion will be situated in an electric field which arises for the most part from the six nearest-neighbor O^{--} ions. The $3d$ electron distribution of the Co^{++} ion is modified from the free-ion case by the crystalline field which splits the $3d$ shell into triply degenerate t_{2g} orbitals and doubly degenerate e_g orbitals. The t_{2g} orbitals have xy, yz, zx symmetry (where x, y, z refer to the cubic axes of the crystal) and the e_g orbitals have $3z^2-r^2$ and x^2-y^2 symmetry. This means that the t_{2g} orbitals are directed along $[hh0]$ axes and e_g orbitals are directed along $[100]$ axes. Thus, the asymmetries, which appear in the measured form factor, will depend on the distribution of the magnetic electrons, i.e., the unpaired electrons over these orbitals or on the value of x in the expression of the form factor for any reflection (h,k,l) given by

$$f=f_s+f_{AS}=f_s+xfe+(1-x)f_t, \qquad (1)$$

where f_s is the spherically symmetric form factor, f_{AS} is the correction applied to f_s due to the anisotropy of the magnetic electron distribution in the crystal, and the f_e and f_t terms are the asymmetric form factors for the unpaired electrons of the type $e_g(x=1)$ or for the type $t_{2g}(x=0)$, respectively.[1] If the unpaired electron density of the ion is a mixture of e_g and t_{2g} electrons, x will have a value between one and zero equal to the fractional occupation of the e_g orbitals.

The values of f_s for four sets of peaks, each set belonging to the same value of $(\sin\theta)/\lambda$, were calculated for different values of x, utilizing Eq. (1), the experimental values of f, and expressions for f_e and f_t given by Weiss and Freeman[1] (Table V). Since f_s should be a monotonic function, the values of the two members of a set should coincide. Table V shows that the column for $x=\frac{2}{3}$ gives the best fit. Hence, 33% of the unpaired electrons are in the t_{2g} orbital and 67% in the e_g orbital. The distribution of the $3d$ electrons of the Co^{++} ion over the different orbitals in a crystal field is demonstrated diagrammatically in Fig. 3. This agrees with the ground-state configuration assigned by Pratt and

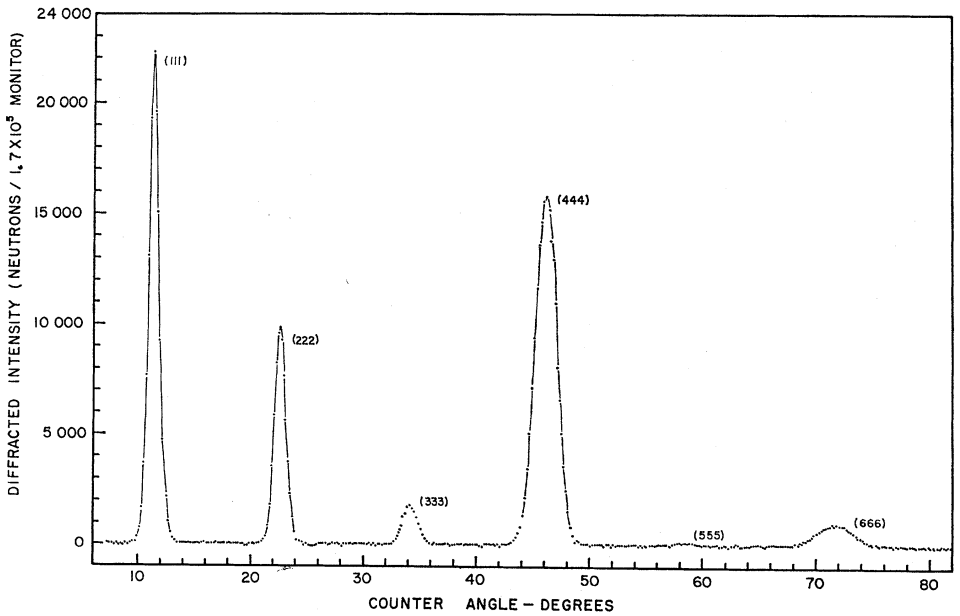

FIG. 2. Typical neutron-diffraction pattern of CoO.

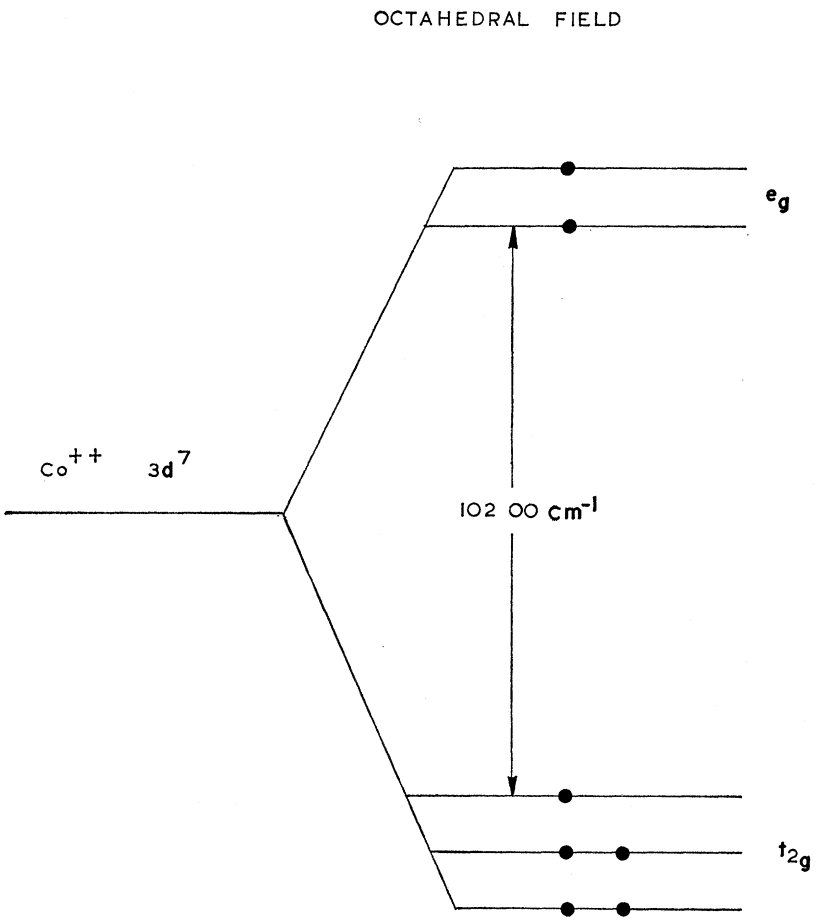

FIG. 3. Distribution of the *3d* electrons of the Co^{++} ion over the orbitals in an octahedral crystal field. Each full circle represents an electron.

Coelho[25] from their optical-absorption-spectrum studies of CoO.

SPHERICAL MAGNETIC FORM FACTOR: RESULTS AND DISCUSSION

The values of f_s, the spherically symmetric magnetic form factor, for different peaks for thermal vibration factor $2B=1.00\times10^{-16}$ cm^2 are listed in Table VI. The values of f_s are displayed against $(\sin\theta)/\lambda$ in Fig. 4. The experimental points were compared with the theoretical symmetric free-ion factor of Freeman and Watson.[2] A reasonable fit to data required a 17% expansion of the free-ion curve along the $(\sin\theta)/\lambda$ scale, which is equivalent to the compression of charge density by about 15%. The expansion of the spherically symmetric magnetic form factor of Co^{++} ion with respect to the theoretical free-ion form factor of Freeman and Watson is evident in the result of Scatturin *et al.*[26] also, who derived it from the neutron-diffraction data for Co^{++} in $KCoF_3$ over a range of $(\sin\theta)/\lambda$ from 0 to about 0.5. It is in-

TABLE V. Comparison of f_s values of "doublets" for various values of x.

Peak	$(\sin\theta)/\lambda$	f_s $x=0$	$x=\frac{1}{3}$	$x=\frac{2}{3}$	$x=1$
333	0.305	0.52	0.54	0.55	0.57
151	0.305	0.59	0.58	0.565	0.55
515	0.421	0.35	0.37	0.38	0.39
$\bar{1}17$	0.421	0.45	0.42	0.38	0.35
775	0.654	0.08	0.12	0.16	0.20
1, 1, 11	0.654	0.29	0.22	0.15	0.08
993	0.771	0.01	0.04	0.07	0.10
1, 1, 13	0.771	0.24	0.17	0.10	0.03

TABLE VI. Isotropic magnetic form factor of Co^{++} ion.

Peak	$(\sin\theta)/\lambda$	f_s	Peak	$(\sin\theta)/\lambda$	f_s
111	0.102	0.90±0.02	373	0.482	0.31±0.01
311	0.195	0.77±0.02	555	0.509	0.27±0.01
113	0.195	0.76±0.02	119	0.537	0.23±0.01
313	0.257	0.65±0.01	377	0.609	0.16±0.01
333	0.305	0.55±0.01	775	0.654	0.16±0.01
$\bar{3}33$	0.305	0.55±0.01	1, 1, 11	0.654	0.15±0.01
151	0.305	0.57±0.01	777	0.713	0.12±0.03
515	0.421	0.38±0.01	993	0.771	0.07±0.03
155	0.421	0.38±0.01	1, 1, 13	0.771	0.10±0.03
$\bar{1}17$	0.421	0.38±0.01	1, 1, 15	0.889	0.03±0.04
733	0.482	0.31±0.01	...	...	...

[25] G. W. Pratt and R. Coelho, Phys. Rev. **116**, 281 (1959).

[26] V. Scatturin, L. Corliss, N. Elliot, and J. Hastings, Acta Cryst. **14**, 19 (1961).

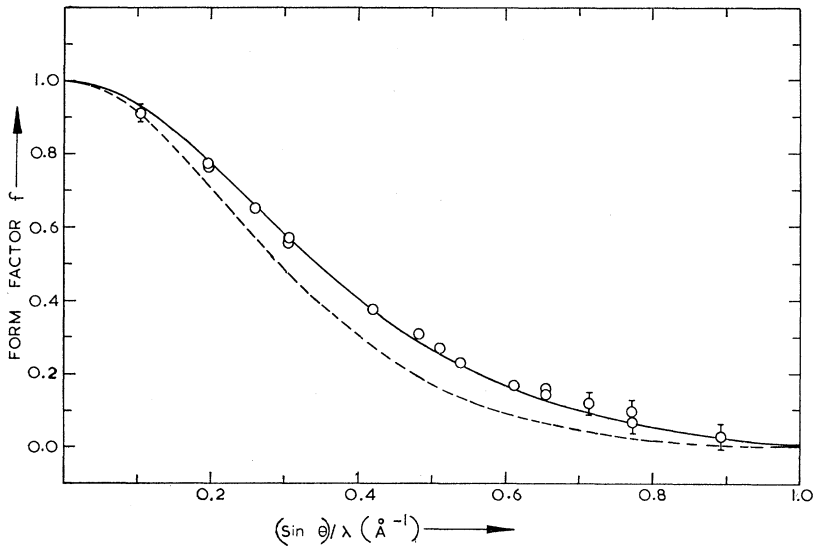

FIG. 4. Plot of the experimentally determined spherically symmetric magnetic form factor against $(\sin\theta)/\lambda$. For comparison, the theoretical form factor for the free Co^{++} ion (dashed curve) and the curve obtained by a 17% expansion along $(\sin\theta)/\lambda$ (full-line curve) are plotted. The Debye-Waller thermal-vibration factor $2B=1.00\times10^{-16}$ cm² is used.

teresting to note that a better fit of the magnetic data was obtained with $2B=0.46\times10^{-16}$ cm², i.e., the value at 77°K (Fig. 5). The expansion along $(\sin\theta)/\lambda$ was now 15% which corresponds to a charge-density contraction of 13%.

Watson and Freeman[27] have investigated the spin-density contraction effects in a Ni^{++} ion when put in a cubic crystalline field. Extending their arguments to the case of the Co^{++} ion in the crystalline field, one reaches the conclusion that the cubic field expands the five t_{2g} electrons and compresses the two e_g electrons. This results in a slightly expanded average form factor. Again, due to the spin polarization effect[27,28] there is a net negative spin density in the regions close to the nucleus and at large radii balanced by a positive spin-density distribution of equal magnitude in the central region. This leads to a positive contribution to the magnetic scattering, with a consequent expansion of the form factor. As for the $3d$ electrons, the t_{2g} electrons with spin-up are contracted relative to the t_{2g} electrons with the spin-down and the two unpaired e_g electrons are also compressed, both leading to an expansion of the form factors. Under the combined effect of the crystalline field and the spin polarization, the form factor is expanded from its free-ion value by approximately 4%.

The expansion of the form factor is also partially accounted for by the presence of the orbital angular momentum producing a maximum magnetic field and hence neutron scattering around $r=0$. The effective spin of Co^{++} in CoO ($S_{eff}=1.68$) as compared to the spin only value 1.5 bears evidence to the fact that the orbital angular momentum is only partially quenched

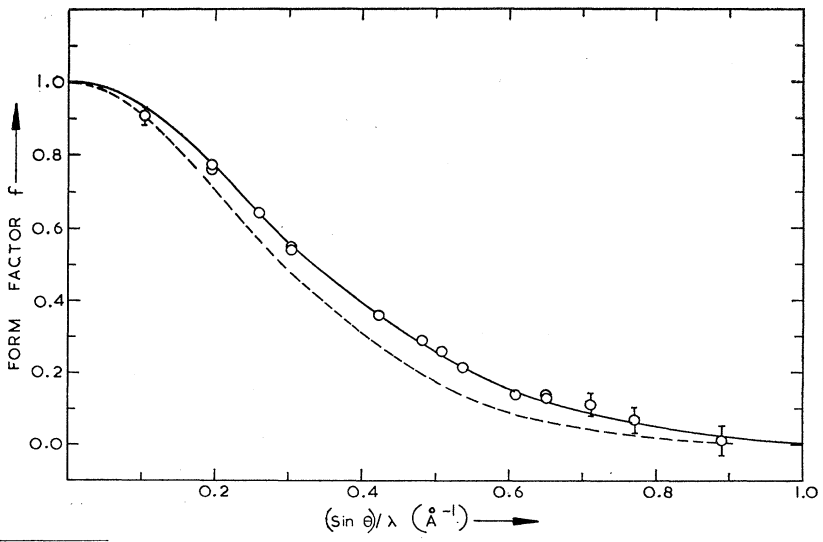

FIG. 5. Plot of the experimentally determined spherically symmetric magnetic form factor against $(\sin\theta)/\lambda$. For comparison, the theoretical form factor for the free Co^{++} ion (dashed curve) and the curve obtained by a 15% expansion along $(\sin\theta/\lambda)$ (full-time curve) are plotted. The Debye-Waller thermal vibration factor $2B=0.46\times10^{-16}$ cm² is used.

[27] R. E. Watson and A. J. Freeman, Phys. Rev. **120**, 1134 (1960).
[28] R. E. Watson and A. J. Freeman, Phys. Rev. **120**, 1125 (1960).

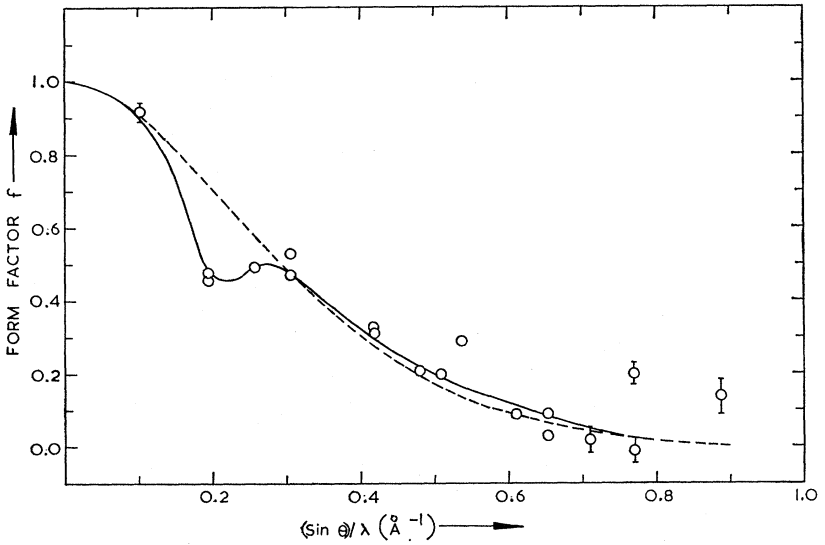

FIG. 6. Plot of the experimentally determined spherically symmetric magnetic form factor against $(\sin\theta)/\lambda$ using Roth's model with angle of deviation 10° from the c axis. For comparison, the theoretical form factor for the free Co^{++} ion is also plotted: $2B=1.00\times10^{-16}$ cm².

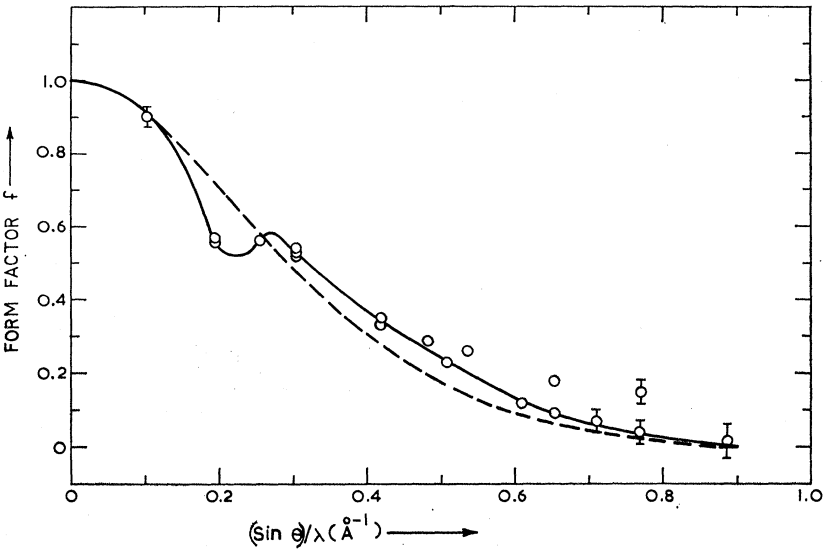

FIG. 7. Plot of the experimentally determined spherically symmetric magnetic form factor against $(\sin\theta)/\lambda$ using Li's model B with an angle of deviation 0° from c axis. For comparison, the theoretical form factor for the free Co^{++} ion is also plotted (dashed curve): $2B=1.00\times10^{-16}$ cm².

in this case. Blume[29] has calculated the expansion of form factor in Ni^{++} due to a partially quenched orbital angular momentum. The study will be more difficult for Co^{++} because of its degenerate ground state. However, his expansion value of 6% may be taken as an approximate value.

Blume could not completely account for the expansion of the free-ion curve in the case of Ni^{++} in NiO. A similar situation exists in the case of the Co^{++} ion in CoO. This necessitates a serious theoretical reconsideration of the mechanisms involved in neutron diffraction in these oxides.

Finally, the spherical magnetic form factors were calculated on the basis of Roth's A model with $\phi=10°$ and Li's model B with $\phi=0°$. Figure 6 compares the form-factor curve based on Roth's model with the theoretical Freeman-Watson curve. Figure 7 compares the form-factor curve based on Li's model B with the Freeman-Watson curve. For both models there is an enormous distortion of the experimental curve in the range $(\sin\theta)/\lambda=0.10$–$0.30$ (Figs. 6 and 7). The spin-density distribution required to explain it will have a magnitude at least ten times that of the Freeman-Watson argon-core spin-density distribution[26,27] and defies any theoretical interpretation of its origin. This was considered to be conclusive evidence against these models and in favor of the van Laar model.

[29] M. Blume, Phys. Rev. 124, 96 (1961).

ACKNOWLEDGMENTS

The authors wish to express their sincere thanks to Dr. B. van Laar for his illuminating correspondence with them. One of the authors (D.C.K.) expresses his thanks to Dr. J. Mahanty for an interesting discussion.